Oncogene (2016) **35,** 1445–1456

www.nature.com/onc

ORIGINAL ARTICLE

Eritoran inhibits S100A8-mediated TLR4/MD-2 activation and tumor growth by changing the immune microenvironment

A Deguchi[1], T Tomita[1], U Ohto[2], K Takemura[3], A Kitao[3], S Akashi-Takamura[4], K Miyake[5] and Y Maru[1]

S100A8/A9 is a major component of the acute phase of inflammation, and appears to regulate cell proliferation, redox regulation and chemotaxis. We previously reported that S100A8/S100A9 are upregulated in the premetastatic lung. However, the detailed mechanisms by which S100A8 contributes to tumor progression have not been elucidated. In this study, we investigated the TLR4/MD-2 dependency by S100A8 on tumor progression. We found that S100A8 (2–89) peptide stimulated cell migration in a manner dependent on TLR4, MD-2 and MyD88. The S100A8 (2–89) peptide also activated p38 and NF-κB in TLR4-dependent manner. The peptide induced the upregulation of both IL-6 and Ccl2 in peritoneal macrophages obtained from wild-type mice, but not TLR4-deficient mice. We then investigated the responsible region of S100A8 for TLR4/MD-2 binding by a binding assay, and found that C-terminal region of S100A8 binds to TLR4/MD-2 complex. To further evaluate the TLR4 dependency on tumor microenvironment, Lewis lung carcinoma-bearing mice were treated with Eritoran, an antagonist of TLR4/MD-2 complex. We found that both tumor volume and pulmonary recruitment of myeloid-derived suppressor cells were reduced with the treatment of Eritoran for five consecutive days. Eritoran reduced the development of tumor vasculature, and increased tumor-infiltration of $CD8^+$ T-cells. Taken together, S100A8 appears to play a crucial role in the activation of the TLR4/MD-2 pathway and the promotion of a tumor growth-enhancing immune microenvironment.

Oncogene (2016) **35,** 1445–1456; doi:10.1038/onc.2015.211; published online 13 July 2015

INTRODUCTION

The S100s are a family of over 20 related calcium-binding proteins that are exclusively expressed in vertebrates, and characterized by two calcium-binding EF-hand motifs: a C-terminal EF-hand (high affinity to calcium), and an N-terminal EF-hand (low affinity to calcium) and connected by a central hinge.[1,2] Calcium binding within the EF-hand motif occurs in response to increased intracellular calcium concentrations and causes conformational changes that expose a wide hydrophobic cleft that interacts with target proteins. Like most S100 protein, S100A8 can form as a heterodimer/heterotetramer with S100A9,[3,4] and as a homodimer or monomer.[5–7]

S100A8 and S100A9 are constitutively expressed in neutrophils,[8] myeloid-derived dendritic cells,[9] platelets,[10] osteoclasts, hypertrophic chondrocytes[11] and in trophoblasts in developing embryo.[12] In contrast, these molecules are induced under inflammatory stimuli in monocytes/macrophages,[13,14] microvascular endothelial cells,[15,16] keratinocytes,[17] and fibroblasts.[18] In a mouse model of colorectal cancer metastasis, myeloid-derived cells were accumulating surrounding metastatic foci in the liver.[19]

S100A8/A9 complex is implicated in diverse intracellular signal processes, including dihydronicotinamide-adenine dinucleotide phosphate oxidase activation,[20] and cytoskeleton rearrangement.[21] In addition, S100A8/A9 is secreted via a golgi complex-independent pathway,[22] which exerts endogenous damage-associated molecular patterns.[23]

Toll-like receptors (TLRs), the best characterized family of pattern recognition receptors, were originally characterized for their ability to respond to exogenous pathogen-associated molecular patterns (PAMPs) that include bacterial lipopolysaccharide (LPS), bacterial diacylated and triacylated lipopeptides, bacterial flagellin, bacterial and viral unmethylated CpG-containing DNA motifs and viral single- and double-stranded RNA. In addition to PAMPs, TLRs also recognize damage-associated molecular patterns. Heat-shock protein (Hsp) 60,[24] Hsp70,[25] high-mobility group box 1,[26] S100A8/S100A9,[27] serum amyloid A3 (SAA3),[28,29] Fetuin-A,[30] defensin β,[31] fibrinogen[32] and fibronectin,[33] as well as polysaccharides such as hyaluronan,[34] heparan sulfate,[35] biglycan[36] and decorin[37] appear to be endogenous ligands of TLR4. The ligand-induced dimerization of TLRs triggers the recruitment of adaptor proteins to intracellular TIR (Toll/interleukin-1 receptor) domains to initiate signaling. Signaling cascades via the TIR domains is mediated by specific adaptor molecules, including MyD88, MAL (also known as TIRAP), TRIF and TRAM.[38] TLR4 associates with co-receptor MD-2 and LPS binding to MD-2 induces the dimerization of TLR4.[39] A previous study showed that TLR4 activates the NF-κB pathway through MyD88-dependent signaling as an early-phase regulation and TRIF-dependent signaling as a late-phase regulation.[40] TRIF signaling initially increases transcriptional levels of interferons in an IRF3-dependent manner.[41]

Eritoran is a structural analog of the Lipid A from *Rhodobacter sphaeroides* (RsLA), competitively binds to TLR4/MD-2, which results in inhibition of LPS-induced inflammatory responses. Phases I and II studies showed that Eritoran could inhibit endotoxin challenge-induced cytokine production. LPS-like

[1]Department of Pharmacology, Tokyo Women's Medical University, 8-1 Kawada-cho, Shinjuku-ku, Tokyo, Japan; [2]Graduate School of Pharmaceutical Sciences, The University of Tokyo, Hongo, Bunkyo-ku, Tokyo, Japan; [3]Institute of Molecular and Cellular Biosciences, The University of Tokyo, Tokyo, Japan; [4]Department of Microbiology and Immunology, Aichi Medical University, Nagakute, Aichi, Japan and [5]Division of Infections Genetics, The Institute of Medical Science, The University of Tokyo, Tokyo, Japan. Correspondence: Dr A Deguchi or Dr Y Maru, Department of Pharmacology, Tokyo Women's Medical University, 8-1 Kawada-cho, Shinjuku-ku, Tokyo 162-8666, Japan.
E-Mail:deguchi@research.twmu.ac.jp or ymaru@research.twmu.ac.jp
Received 8 October 2014; revised 30 April 2015; accepted 4 May 2015; published online 13 July 2015

agonist activity has been not reported in human, dogs, rat and mice treated with Eritoran. Eritoran does not directly interact with TLR4, but competes with LPS at the hydrophobic pocket of MD-2.[42]

We previously reported that tumor-derived growth factors such as tumor necrosis factor α (TNFα) and vascular endothelial growth factor induced the expression of two endogenous ligands of TLR4, such as S100A8 and SAA3, in premetastatic lungs, and that SAA3 functions as a TLR4-mediated chemotactic agonist for both myeloid cells and tumor cells.[29] The auto-amplification of SAA3 in lung-specific Club cells may contribute to organotropism in lung metastasis.[43] We more recently reported that SAA3 activates TLR4/MD-2 pathway in a MyD88-dependent, but TRIF-independent manner by using an SAA3 peptide.[28] In contrast, in case of S100A8, RAGE and TLR4 are identified as S100A8/A9 receptors. However, the mechanism(s) which signaling mediated by S100A8 mainly has a role in inflammatory response is still unclear. In this study, using synthetic peptides or mammalian-derived S100A8 recombinant protein, we investigated the role of S100A8 on TLR4/MD-2 activation in tumor progression. We found that C-terminal region of S100A8 has an important role on NF-κB activation through TLR4-medicated signaling, but not through RAGE.

RESULTS

S100A8 (2–89) peptide induces cell migration in a TLR4-dependent manner

Others and we previously demonstrated that S100A8 activate TLR4/MD-2 signaling as an endogenous ligand.[27,44] Although several reports suggested that S100A8 preferentially exist as a heterodimer with S100A9,[3,4] mouse S100A8 can form a homodimer in yeast two-hybrid system.[45] In addition, S100A9 alone can act as an endogenous ligand of TLR4/MD-2.[46,47] Thus, the involvement of S100A8 on TLR4/MD-2 signaling is still unclear. In this study, to confirm S100A8 as a TLR4/MD-2 endogenous ligand more directly, we used synthetic peptide of S100A8.

We first examined the efficacy of the peptide on cell migration. Although the effective dosages of S100A8 (2–89) peptides on cell migration were slightly higher than mammalian cell-derived S100A8 proteins, S100A8 (2–89) peptide at 0.1 μg/ml efficiently enhanced cell migration in RAW264.7 cells (Figure 1a). We also found that S100A8 (2–89) peptide stimulated cell migration in peritoneal macrophages obtained from wild-type mice, but not from *Tlr4*$^{-/-}$, *MD-2*$^{-/-}$ or *MyD88*$^{-/-}$ mice (Figure 1b). These results suggest that S100A8 (2–89) peptide can elicit TLR4/MD-2-mediated cell migration similar to full-length S100A8 protein. We then tested inflammatory cytokine production by S100A8 (2–89) peptide in peritoneal macrophages obtained from wild-type or *Tlr4*$^{-/-}$ mice. As shown in Figure 1c, inflammatory cytokine such as IL-6, Ccl2 and to lesser extent TNFα are upregulated by S100A8 (2–89) peptide.

S100A8 (2–89) peptide binds to TLR4/MD-2. We next performed a binding assay to detect S100A8 binding to TLR4/MD-2. S100A8 (2–89) peptide preferentially not only bound TLR4/MD-2 but also bound MD-2 alone. The *KD* values for TLR4/MD-2 complex or MD-2 were determined to be 0.32 or 0.73 μM, respectively (Figure 2a). To narrow down the binding site of S100A8 on TLR4/MD-2, we made the S100A8 sequence divide into three, subsequently

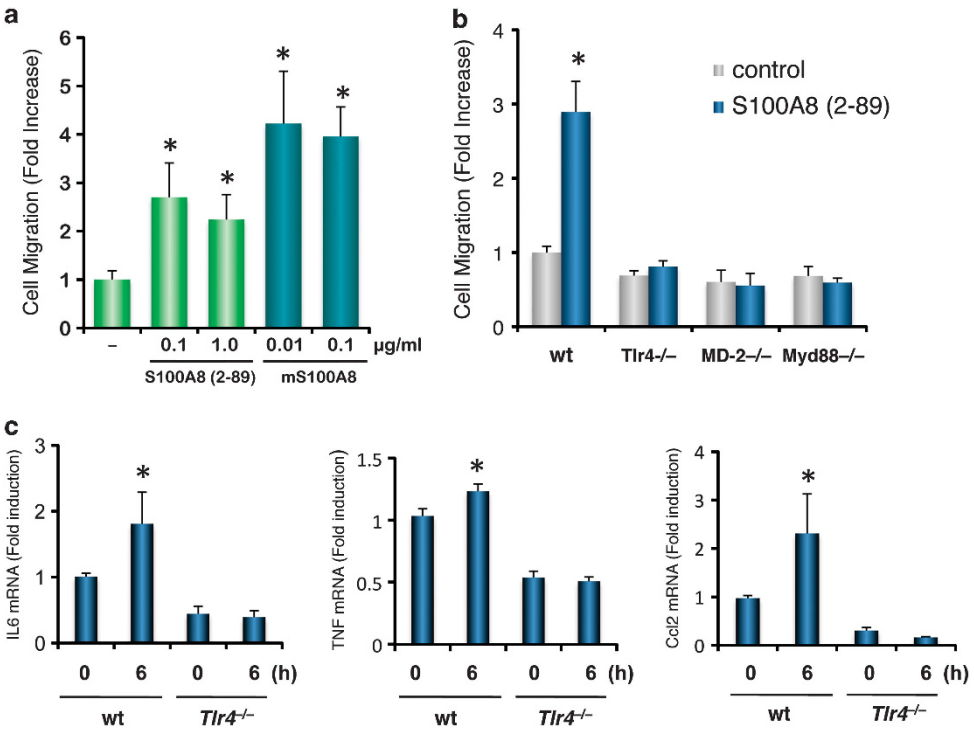

Figure 1. The S100A8 induces cell migration, and inflammatory cytokines expression in peritoneal macrophages or RAW264.7 cells. (**a**) RAW264.7 cells were treated with the indicated concentrations of the peptide or mammalian-derived S100A8 for 6 h. Cells that migrated through the filter were counted by crystal violet staining. (**b**) Peritoneal macrophages were obtained from wild-type vs TLR4, MD-2 or MyD88 knockout mice. These cells were subjected to a cell migration assay in the presence of 0.1 μg/ml (equivalent to 0.01 μM) of S100A8 (2–89) peptide. Data are the mean ± s.d. of nine samples in one representative experiment. Similar results were obtained in three independent experiments. (**c**) S100A8 induces expression of inflammatory cytokine mRNAs in peritoneal macrophages in a TLR4-dependent manner. Peritoneal macrophages were treated with 0.1 μg/ml of S100A8 (2–89) peptide for 6 h. Total RNAs were extracted and quantitative PCR analysis was performed using relevant primer sets and SYBR green. Relative expression levels were compared. The expression of each gene was normalized to actin expression, and fold induction was presented relative to control. *$P < 0.05$ compared with control. Data are the mean ± s.d. ($n = 3$).

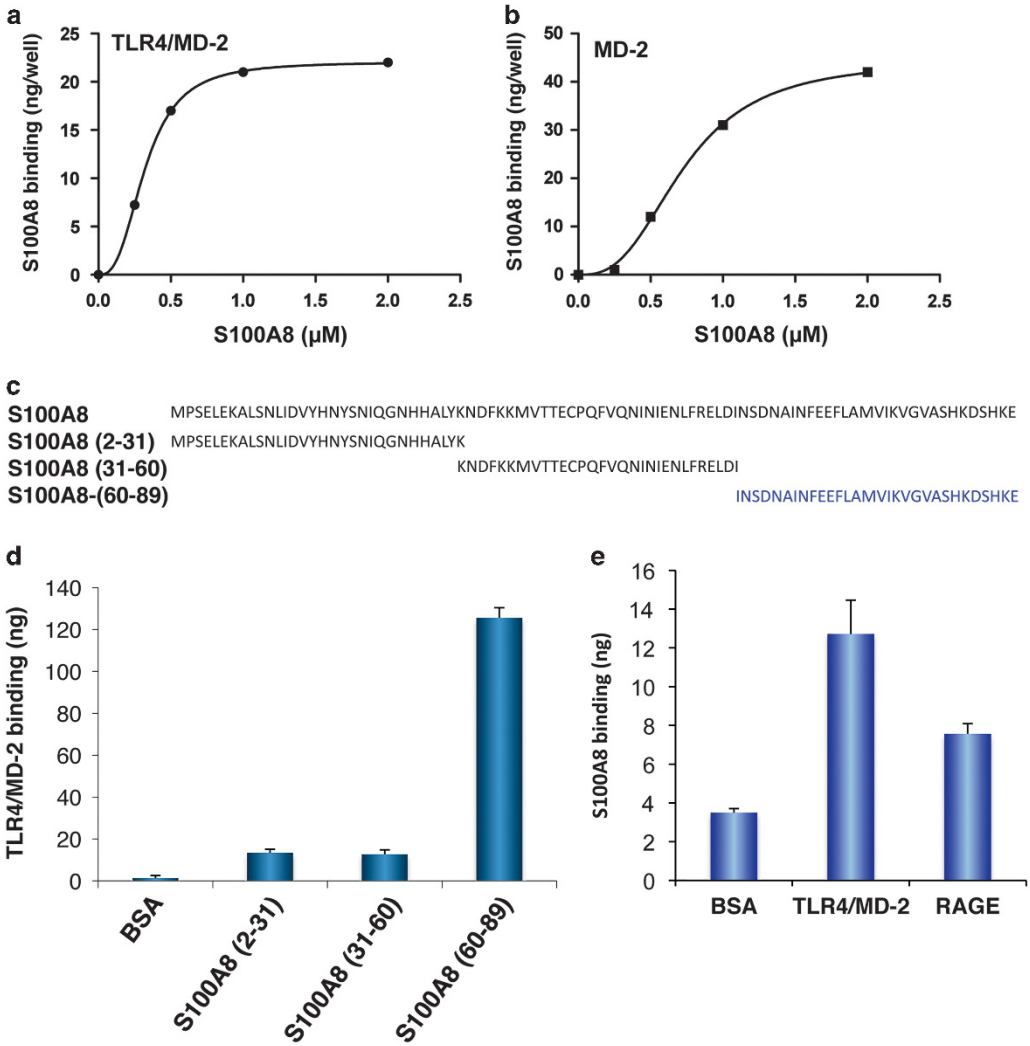

Figure 2. The S100A8 (2–89) peptide binds to TLR4/MD-2, and also MD-2 alone. (**a**) S100A8 (2–89) peptide binds to TLR4/MD-2 complex. TLR4/MD-2 recombinant proteins were coated on the ELISA plate. After blocking, S100A8 (2–89) peptides at various concentrations were added to the plate. The more detailed methods were described in Materials and Methods. Similar results were obtained in three independent experiments. (**b**) S100A8 (2–89) peptide binds to MD-2. MD-2 recombinant proteins were coated on the ELISA plate. After blocking, S100A8 (2–89) peptides at various concentrations were added to the plate. The more detailed methods were described in Materials and Methods. Similar results were obtained in three independent experiments. (**c**) A series of three divided S100A8 synthetic peptides. (**d**) S100A8 (60–89) peptide preferentially binds to TLR4/MD-2 complex. S100A8 (2–31), S100A8 (31–60) or S100A8 (60–89) peptides were coated on the ELISA plate. After blocking, TLR4/MD-2 recombinant protein complex were incubated on the coated plate. The more detailed methods were described in Materials and Methods. (**e**) S100A8 (60–89) peptide binds to TLR4/MD-2, but to a lesser extent to RAGE. TLR4/MD-2 or RAGE recombinant proteins were coated on the ELISA plate. After blocking, S100A8 (60–89) were incubated on the coated plate. The more detailed methods were described in Materials and Methods.

generated synthetic 30-mer peptides (Figure 2c). S100A8 (60–89) peptide bound to TLR4/MD-2 complex, but both S100A8 (2–31) and S100A8 (31–60) failed to bind to TLR4/MD-2 (Figure 2d). S100A8/S100A9 has been also known to bind to RAGE. To investigate whether the binding site of S100A8 upon TLR4 is similar region to RAGE or not, we next examined whether the S100A8 (60–89) peptide binds to TLR4/MD-2 or RAGE recombinant protein by performed a receptor-coated enzyme-linked immunosorbent assay (ELISA). S100A8 (60–89) binds to TLR4/MD-2 stronger than the binding to RAGE (Figure 2e).

To investigate interactions between TLR4/MD-2 and S100A8, we generated the complex structure models from the crystal structures of TLR4/MD-2 monomer and S100A8 dimer by the combination of rigid-body docking program ZDOCK3 and clustering/reranking method CyClus.[48] The structures and the interface residues of the obtained top five models are shown in Figure 3 and Table 1, respectively. In all the models, the C-terminal residues are located on the interface with TLR4/MD-2, which supports the experimental results in Figure 1. These results suggest that C-terminal region of S100A8 has a crucial role in binding of TLR4/MD-2.

Eritoran inhibits S100A8-mediated cell migration, p65 and p38 phosphorylation

We further investigated the TLR4 dependency on S100A8 using a TLR4 antagonist, Eritoran. Lewis lung carcinoma (LLC) cells were pretreated with various concentrations of Eritoran, and then added S100A8 with the indicated concentration into the lower well of culture insert in the presence/absence of Eritoran. The pretreatment of Eritoran diminished S100A8-induced cell migration in an Eritoran dose-dependent manner (Figure 4a).

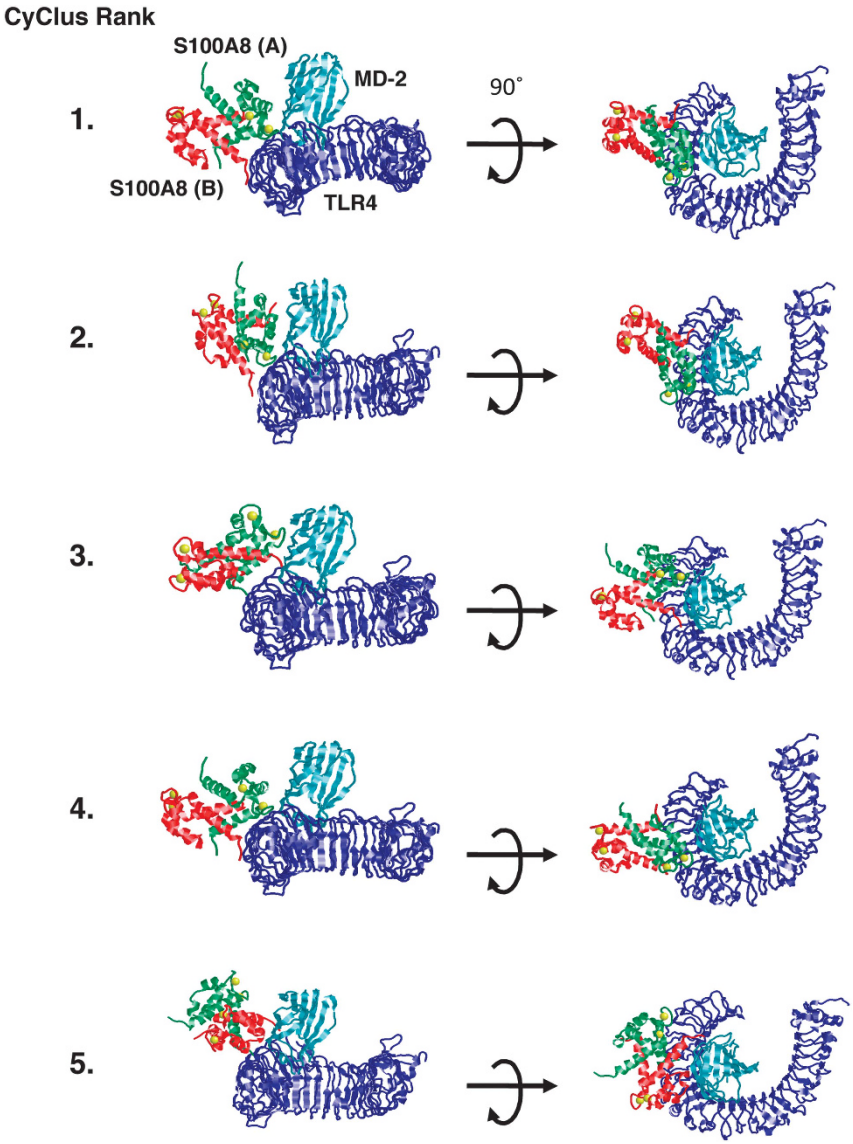

Figure 3. Five model structures of TLR4/MD-2-S100A8 determined by the computational simulation (CyClus). The left five structures present the top view of the complexes, and the 90° rotation of each complex (the side view) is shown in the right panel. Structural data for TLR4 (blue) and MD-2 (cyan) is taken from PDB: 2Z64, and data for S100A8 homodimer (chain A = green, chain B = red) is obtained from PDB: 1MR8.

Eritoran also inhibited SAA3-induced cell migration (Supplementary Figure 1), suggesting that Eritoran can block endogenous TLR4 ligands-induced cell migration. The authentic TLR4 ligand, LPS, was shown to activate the p38, JNK, ERK pathway.[49] These mitogen-activated protein kinases are known to be upstream of NF-κB signaling.[50] We then examined the time dependency of p38 activation by S100A8 (2–89) peptide, and found that both p38 and p65 phosphorylation significantly increased after 30 min (Figure 4b) in LLC cells with the S100A8 (2–89) peptide treatment. In contrast, Eritoran perfectly blocked S100A8-induced p65 phosphorylation as well as p38 phosphorylation (Figure 4b). The similar results were obtained from RAW264.7 cells (Supplementary Figure 2). We also performed the pNF-κB-Luc reporter assay to determine the effect of Eritoran on S100A8-mediated NF-κB activation. As shown in Figure 4c, Eritoran blocked S100A8-induced NF-κB activation. Furthermore, we performed the competition assay to determine whether S100A8 could compete with Eritoran. The *Ki* values of Eritoran against SAA3 and S100A8 were calculated as 15 and 45 nM, respectively (data not shown). These results suggest that Eritoran inhibits S100A8-induced cell migration, and both p38 and NF-κB activation through direct blocking of TLR4/MD-2.

Eritoran inhibits tumor growth in tumor-bearing mice through inhibiting angiogenesis

Myeloid-derived suppressor cells (MDSCs) appear to infiltrate surrounding primary tumor.[51,52] S100A8/S100A9 produced by immune cells is known to contribute to establish tumor-favorable microenvironment.[53] In addition to the role of S100A8 in the tumor microenvironment, the upregulation of S100A8 is observed in premetastatic lung,[44] which involved into the accumulation of myeloid cells in lungs from bone marrow. The treatment of LPS accelerates tumor progression in experimental colorectal cancer mouse models.[54] To confirm whether blockage of TLR4/MD-2 could reduce tumor progression, we examined the treated tumor-bearing mice with Eritoran following a protocol as shown in Figure 5a. The treatment of Eritoran for five consecutive days significantly reduced the tumor volume (Figure 5b) and tumor vasculature, indicating that Eritoran inhibited angiogenesis

Table 1. Possible interface residues of TLR4/MD-2/human S100A8 dimer

Id	*Interface residues*
1	TLR4(21) Q114 K136 A138 S139 E141 S142 H158 N159 F160 H162 S163 T183 N184 T185 Q187 L211 N212 P213 D264 E265 R266 MD2(6) H62 E64 T112 N114 T115 S116 ChainA(19) N10 D14 V15 H17 K18 T19 S20 L21 I22 K23 G24 N25 F26 H27 T30 D32 D33 K36 E39 ChainB(5) S86 H87 E88 E89 S90
2	TLR4(26) E90 Q114 S115 F116 K136 A138 S139 S142 F143 H158 N159 F160 H162 T183 N184 T185 I186 Q187 S210 L211 N212 P213 N237 D264 E265 R266 MD2(15) Q21 S45 S47 S48 E49 H62 V63 E64 F65 S103 T112 V113 N114 T115 S116 ChainA(25) L2 N10 I13 D14 H17 K18 T19 S20 L21 I22 K23 G24 N25 F26 H27 A28 T30 D32 D33 K35 K36 L37 E39 T40 E41 ChainB(7) M1 K85 S86 H87 E88 E89 S90
3	TLR4(12) K66 I67 E88 E90 T91 P112 K136 F160 H162 T185 Q187 E265 MD2(17) Q21 Q22 W23 T34 T36 K41 P43 I44 S45 I46 E49 F60 H62 E64 F65 N114 S116 ChainA(15) M1 L2 K7 S11 H17 K18 L21 I22 K23 G24 N25 F26 T30 T40 CA102 ChainB(10) M1 L2 T3 E4 K7 S86 H87 E88 E89 S90
4	TLR4(29) K66 R86 E90 P112 Q114 E134 K136 A138 H158 N159 F160 H162 S163 K165 T183 N184 T185 Q187 T188 T190 N192 D193 L211 N212 P213 G234 N237 E265 R266 MD2(5) H62 E64 N114 T115 S116 ChainA(23) K7 N10 S11 I12 I13 D14 V15 T16 H17 K18 T19 S20 L21 I22 K23 G24 N25 F26 H27 D32 D33 K36 E41 ChainB(9) M1 L2 E4 K7 S86 H87 E88 E89 S90
5	TLR4(18) D41 F62 E134 K136 H158 N159 F160 T183 N184 T185 L211 P213 N237 D264 E265 R266 N267 E269 MD2(18) W23 T36 K41 F42 P43 I44 S45 E49 F60 H62 V63 E64 I66 R68 N114 T115 S116 I117 ChainA(6) M1 L2 T3 E4 E6 K7 ChainB(17) K35 K36 E39 T40 P43 Q44 T45 I46 R47 K48 K49 A81 K84 K85 E88 E89 S90

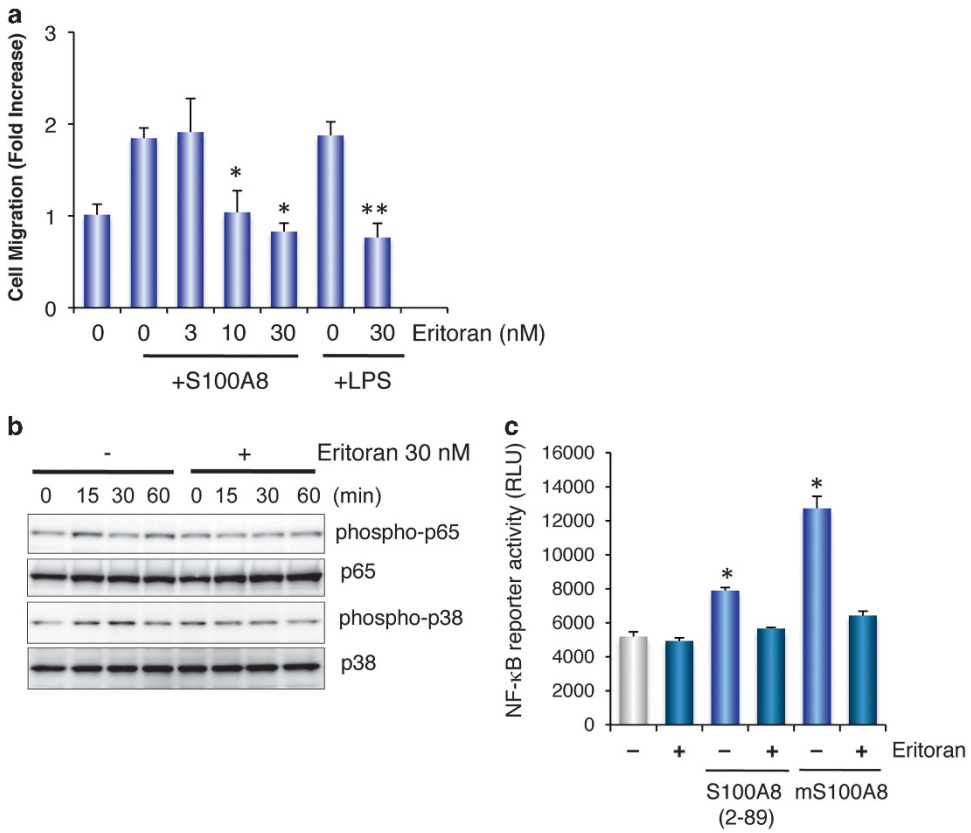

Figure 4. Eritoran inhibits S100A8 (2–89) peptide-mediated cell migration, p38, and NF-κB activation. (**a**) The LLC cells were pretreated with the indicated concentrations of Eritoran, and then seeded into the upper well. S100A8 with the indicated concentration were added into lower well of culture insert in the presence/absence of Eritoran. LPS (100 ng/ml) was used as a positive control. Cells that migrated through the filter were counted by crystal violet staining. Data are the mean ± s.d. of nine samples in one representative experiment. (**b**) LLC cells were pretreated with 30 nM of Eritoran, and then stimulated with S100A8 (2–89) peptide for the indicated times. Cell lysates were subjected to western blotting using the indicated antibody. (**c**) pNF-κB-Luc-LLC reporter cells were pretreated with 30 nM of Eritoran, and then stimulated with S100A8 (2–89) peptide or mammalian-derived S100A8 for 16 h. The luc reporter activities were determined. Data are the mean ± s.d. $^*P < 0.05$ compared with control. Similar results were obtained in three independent experiments.

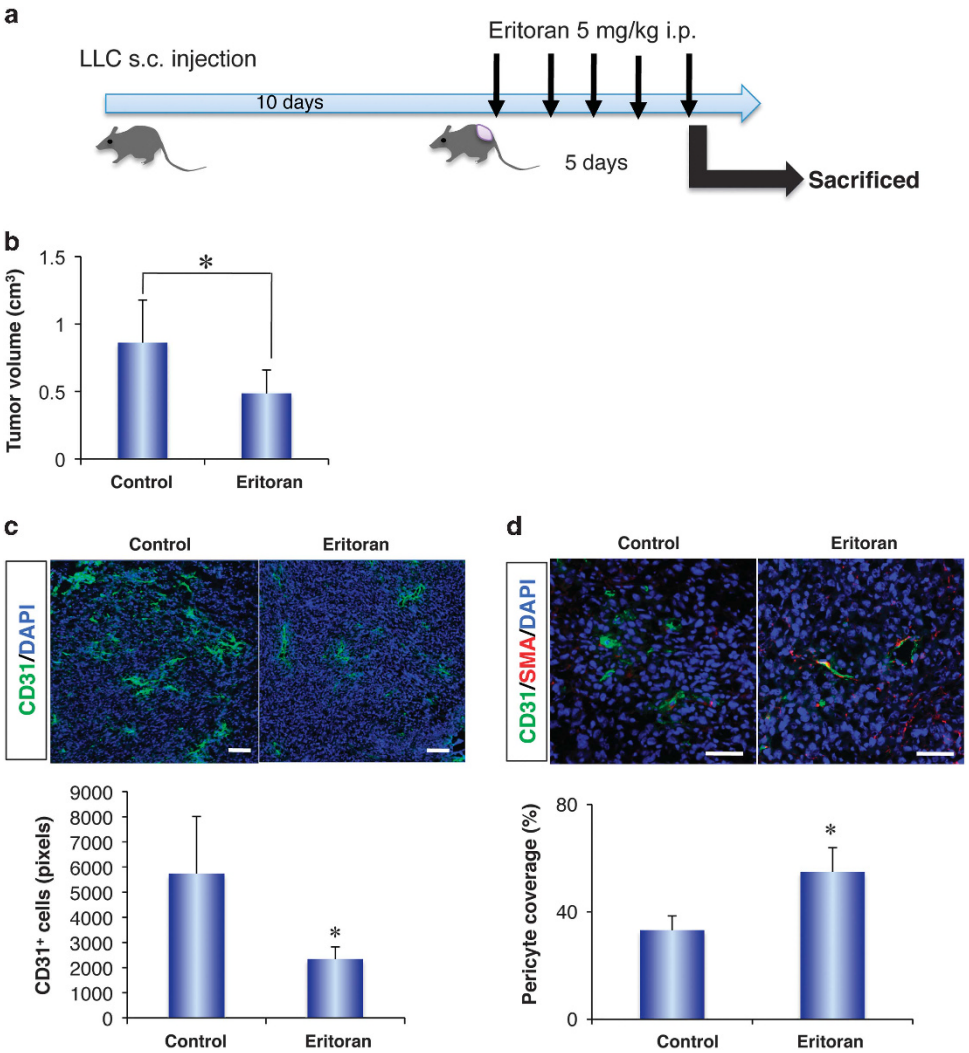

Figure 5. Eritoran blocks tumor progression in LLC-bearing mice. (**a**) An experimental protocol used to test Eritoran in tumor-bearing mice. Briefly, cells were subcutaneously implanted into C57BL6 mice. Post 10 days, tumor-bearing mice started to receive Eritoran (5 mg/kg, i.p.) once daily for five consecutive days. (**b**) The volumes of LLC tumor are reduced by Eritoran. After five consecutive days, mice were killed. The tumor volume was calculated by the formula Tumor volume = 1/2(length × width^2). Data are the mean ± s.d. ($n = 4$–5 mice per group). *$P < 0.05$ compared with control tumor-bearing mice. (**c**) The tumor vasculatures were stained with an anti-CD31 antibody. The representative photos were shown (scale = 100 μm). Pericyte coverage was calculated the signal of α-smooth muscle actin divided with the signal of CD31. The representative photos are shown (scale = 50 μm). *$P < 0.05$ compared with control tumor-bearing mice.

(Figure 5c). In addition, pericyte coverage was markedly increased by Eritoran (Figure 5d). Although Eritoran reduced the tumor volumes of LLC in tumor-bearing mice (Figure 5b), Eritoran did not affect LLC cell proliferation *in vitro* in the absence of any endogenous ligand of TLR4 (data not shown). We next examined the effect of Eritoran on tumor growth in other tumor cell lines. The 4T1- or E0771-expressed endogenous TLR4/MD-2, the expression level of TLR4/MD-2 in each cell line was similar to LLC cells (Supplementary Figures 3A and C). Eritoran also suppressed tumor growth *in vivo* in both 4T1 and E0771 cells (Supplementary Figures 3D and E).

To further confirm the involvement of TLR4 on tumor growth, we generated TLR4 knockdown LLC cells. The knockdown of TLR4 in LLC markedly reduced tumor growth *in vivo*, but not *in vitro* (Supplementary Figure 4).

These results suggest that activation of TLR4 of tumor cells positively regulates tumor microenvironments, through producing pro-inflammatory cytokines. Interestingly, the treatment by Eritoran reduced cellular levels of SAA3, one of downstream targets of TLR4 (Figure 6e).

Bone marrow-derived myeloid cells (that is, tumor-associated macrophages (TAMs, MDSCs) were known to suppress T-cell function, and regulate tumor vasculatures.[55,56] We next tested the effect of Eritoran on the population of tumor-associated macrophages, T-cell populations. The treatment of Eritoran reduced TAMs and $CD11b^+Ly6C^{++}Ly6G^-$ populations (Figures 6a and b). Conversely, the treatment significantly increased tumor infiltrating $CD8^+$ T-cells compared with the control, to a lesser extent, also $CD4^+$ T-cells (Figures 6c and d). Suppression of T-cell function by MDSC more likely depends on Arginase-1 expression. Thus, we examined the mRNA levels of Arginase-1 in intratumoral TAMs, $CD11b^+Ly6C^+Ly6G^+$ and $CD11b^+Ly6C^{++}Ly6G^-$ cell population. Eritoran reduced expression of Arginase-1 in TAMs, to a lesser extent, in both $CD11b^+Ly6C^+Ly6G^+$ and $CD11b^+Ly6C^{++}Ly6G^-$ cell populations (Supplementary Figure 5).

MDSCs also appear to contribute to a premetastatic niche in distant organs.[29,57] As shown in Figure 7a, Eritoran inhibited the pulmonary recruitment of both $CD11b^+Ly6C^+Ly6G^+$ and $CD11b^+Ly6C^{++}Ly6G^-$ cell population, and also inhibited both S100A8 and SAA3 induction in lungs of tumor-bearing mice

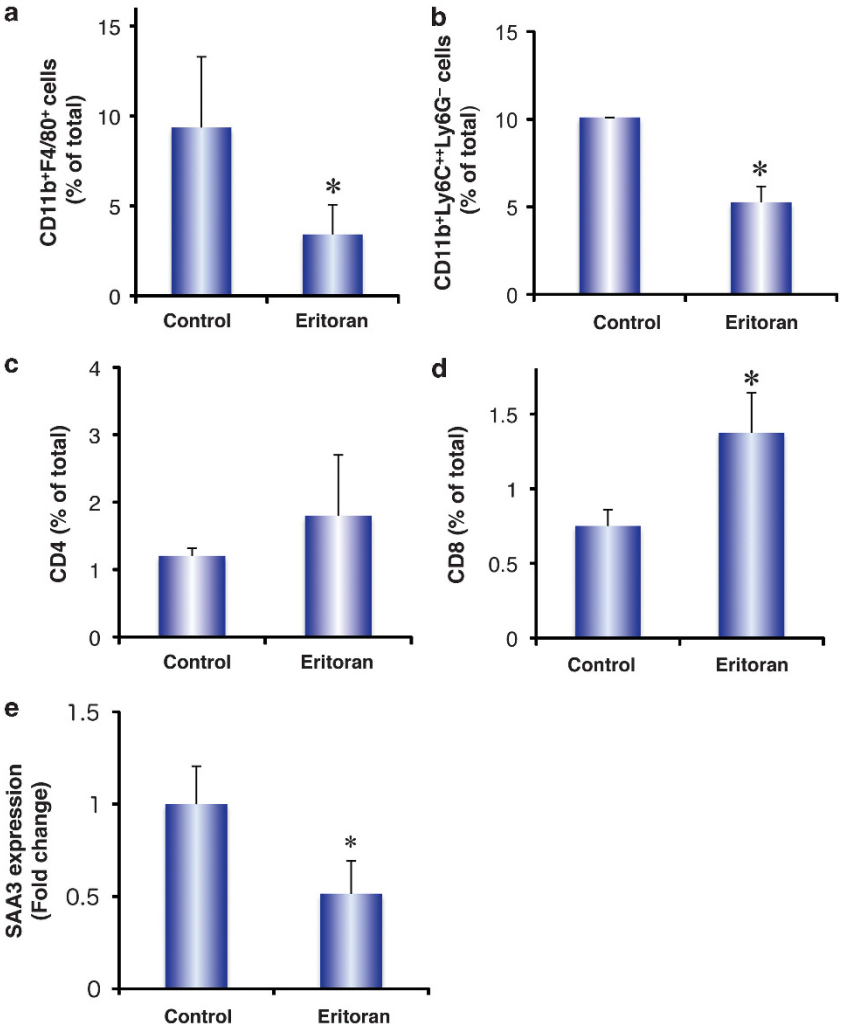

Figure 6. Eritoran suppresses the infiltration of TAMs, and increased intratumoral T-cells infiltration. The effect of Eritoran reduced the intratumoral infiltration of (**a**) TAMs, (**b**) $CD11b^{+}Ly6C^{++}Ly6G^{-}$ cells, (**c**) $CD4^{+}$ T and (**d**) $CD8^{+}$ T-cell populations. Each population was determined by flow cytometry. Data are the mean ± s.d. ($n = 6$ mice per group). *$P < 0.05$ compared with control tumor-bearing mice. (**e**) Eritoran reduced intratumoral SAA3 expression in LLC-bearing mice. Data are the mean ± s.d. ($n = 6$ mice per group). *$P < 0.05$ compared with control tumor-bearing mice.

(Figure 7b). Because S100A8 is one of the endogenous ligands of TLR4/MD-2, we further examined whether the blockage of S100A8 by anti-S100A8 neutralizing antibody is similar to the effects of Eritoran on tumor microenvironment. As expected, the treatment of anti-S100A8 neutralizing antibodies suppressed tumor growth in LLC tumor-bearing mice, and the recruitment MDSC in both primary tumor sites and lungs (Figure 8).

Taken together, these results indicate that Eritoran suppresses tumor microenvironment, which can cause the inhibition of development of premetastatic microenvironment in lungs.

DISCUSSION

In the present study, we found that C-terminal region of S100A8 has a crucial role in TLR4/MD-2 activation, and that blockage of TLR4 signaling by Eritoran can suppress that establishment of tumor microenvironment in both primary tumor site and lungs.

Vogl *et al.*[27] previously reported that S100A8-mediated cytokine induction was mediated by TLR4, not by RAGE, and that S100A9 negatively regulate the binding to TLR4. Our study is consistent with these findings. However, it has been still unknown how S100A8 and S100A8/S100A9 complex binds to TLR4/MD-2 complex.

To date, various molecule can act as agonists of TLR4. The responsible sites of murine MD-2 for LPS are different from the sites for taxol[58] as a TLR4 agonist, suggesting that there are several modes of conformations to activate TLR4/MD-2 complex. Among known TLR4 agonists, high-mobility group box 1 is originally identified as an alarmin, known as an endogenous ligand of TLR4/MD-2. Yang *et al.*[26] that the Cys 106 of high-mobility group box 1 is crucial to bind to TLR4/MD-2 complex. We previously confirmed that murine SAA3 is an endogenous ligand of TLR4/MD-2 using SAA3 (20–86) peptides.[28] In case of SAA3, MD-2 is crucial for SAA3 binding to TLR4/MD-2.[28] As shown in Figure 2b, the results suggested that S100A8 also bound to MD-2, but the molecular docking simulation indicated that S100A8 is likely to bind to TLR4 directly, and that the involvement of MD-2 seems to be lesser extent than the case of SAA3 (Figure 3, and Table 1). Thus, both SAA3 and S100A8 functions as endogenous TLR4 ligand, but the binding style of S100A8 might be different from that of SAA3. S100A8 preferentially not only forms a heterodimer/heterotetramer with S100A9[3,4] but also exists as a homodimer or monomer in clinical settings.[5–7]

S100A8/A9 has been shown to induce anti-tumor responses in the range of 20–250 μg/ml (1–12.5 μM), whereas at lower levels (< 20 μg/ml) S100A8/A9 seems to promote proliferation of tumor

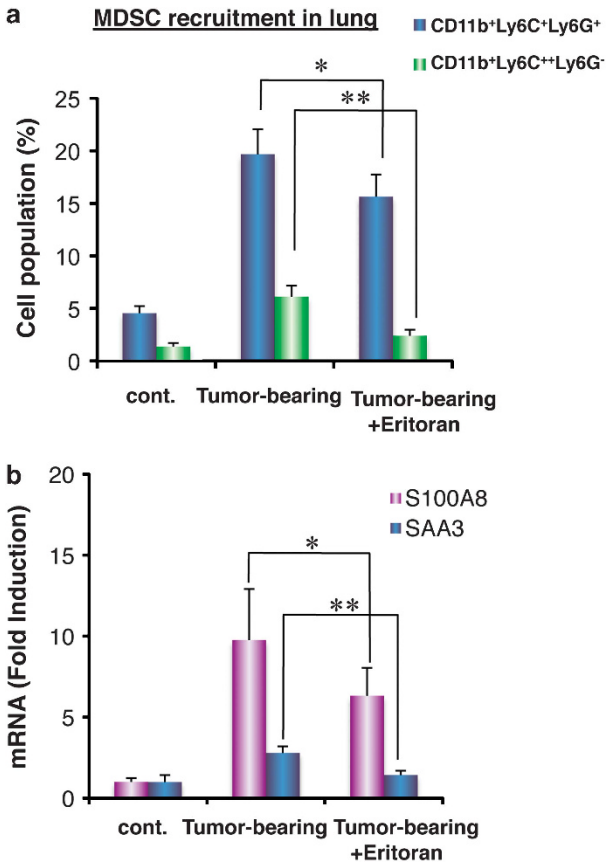

Figure 7. Eritoran suppresses pulmonary recruitment of MDSCs. (**a**) The pulmonary recruitment of MDSCs significantly reduces in tumor-bearing mice treated with Eritoran compared with control (5% dextrose alone). $^{*}P < 0.05$, $^{**}P < 0.01$ compared with tumor-bearing mice. Data are the mean ± s.d. ($n = 4$–5 mice per group). (**b**) Eritoran reduces the expression of S100A8/SAA3 mRNAs in lungs. Total RNAs from lungs were extracted, and quantitative PCR analysis was performed using relevant primer sets and SYBR green. Relative expression levels were compared. The expression of each gene was normalized to actin expression, and fold induction was presented relative to control. Data are the mean ± s.d. ($n = 3$). Similar results were obtained in three independent experiments. $^{*}P < 0.05$, $^{**}P < 0.01$ compared with tumor-bearing mice.

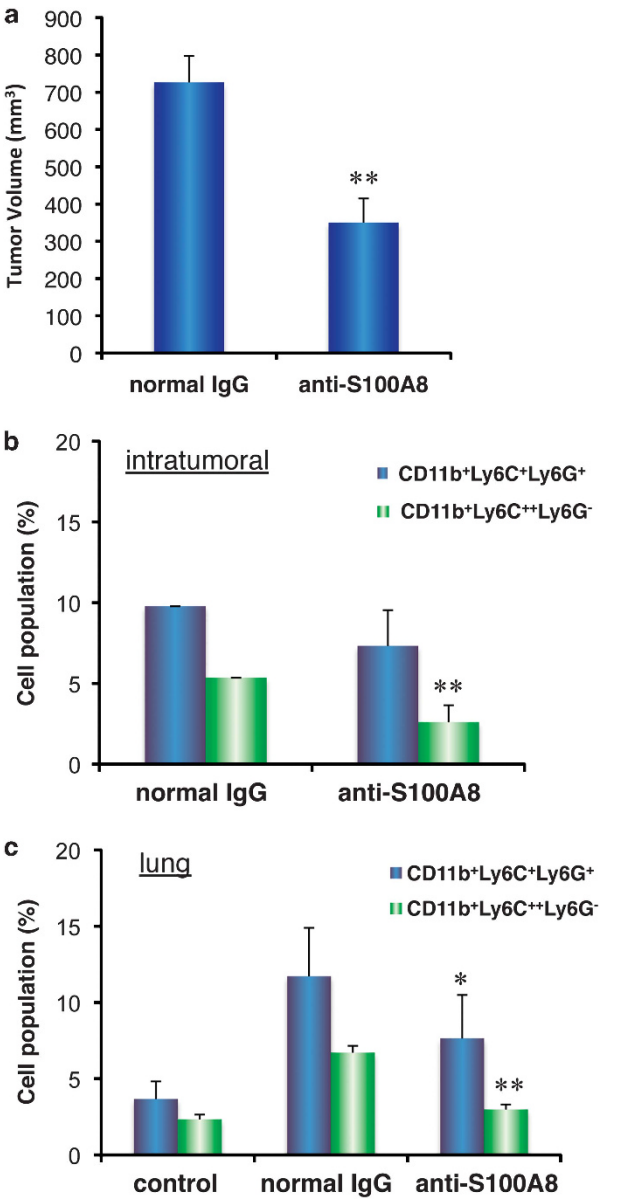

Figure 8. Blockage of S100A8 by anti-S100A8 neutralizing antibodies suppresses tumor microenvironment. (**a**) The volumes of LLC tumor are reduced by anti-S100A8 neutralizing antibodies. The tumor volume was calculated by the formula Tumor volume = 1/2 (length ± width^2). Data are the mean ± s.d. ($n = 6$ mice per group). $^{**}P < 0.01$ compared with normal IgG-treated tumor-bearing mice. (**b**) The treatment of anti-S100A8 neutralizing antibodies reduces the intratumoral recruitment of CD11b$^+$Ly6C^{++}Ly6G$^-$ cell population. Data are the mean ± s.d. ($n = 6$ mice per group). $^{**}P < 0.01$ compared with normal IgG-treated tumor-bearing mice. (**c**) The treatment of anti-S100A8 neutralizing antibodies reduces the pulmonary recruitment of both CD11b$^+$Ly6C^{++}Ly6G$^-$ and CD11b$^+$Ly6C$^+$Ly6G$^+$ cell population. Data are the mean ± s.d. ($n = 6$ mice per group). $^{*}P < 0.05$, $^{**}P < 0.01$ compared with normal IgG-treated tumor-bearing mice.

cells.[59] In addition, while the proapoptotic effect of S100A8/A9 appears to be RAGE-independent, the effects on tumor proliferation are mediated by RAGE, and involve induction of MAPK signaling and NF-κB activation. S100A8/S100A9 complex promotes colon tumor progression via RAGE-dependent pathway in colon cancer,[53] and in colitis-associated carcinogenesis.[60] Thus, S100A8/S100A9-dependent RAGE activation leads to tumor progression.

Since monomeric or homodimeric S100A8 can be found in clinical setting,[5–7] we speculate that S100A8 itself can activate TLR4/MD-2 signaling through the C-terminal region of S100A8.

To confirm the involvement of TLR4 on S100A8-induced p38, and p65 phosphorylation, we pretreated Eritoran before stimulation of S100A8. Eritoran completely abolished both p38 and p65 phosphorylation (Figure 4b). Moreover, the binding of S100A8 (2–89) peptide to TLR4/MD-2 was competitively inhibited by Eritoran, suggesting that the biding site would be similar to LPS upon TLR4/MD-2 binding.

TLR4 activation is known to enhance tumor progression in colon, ovarian, breast cancers and head and neck squamous cell carcinomas.[54,61–63] In contrast, LPS also inhibits tumor growth.[64] Therefore, it was of interest to test the effect of Eritoran on tumor-bearing mice. We found that Eritoran inhibited tumor progression *in vivo* (Figure 5b, and Supplementary Figures 3D and E). The reduction of tumor volume is likely due to reduction of the tumor vasculature, vascular normalization and reduction of both TAMs and CD11b$^+$Ly6C^{++}Ly6G$^-$ myeloid-derived cells infiltration (Figures

5c and 6a). Increased $CD8^+$ T-cell tumor infiltration by Eritoran was presumably due to vascular normalization and/or suppression of TAMs infiltration. Shi *et al.*[65] recently reported that the inflammatory monocytes ($Ly6C^{high}CCR2^+$) recruit from bone marrow upon TLR4 stimulation. Because we showed that Eritoran reduced the recruitment of bone marrow-derived cells in both primary tumor sites and lungs, it is likely Eritoran can inhibit the recruitment of bone marrow-derived myeloid cells. More recently, Qin *et al.*[66] reported that the peptibody depletes MDSC, which suppresses tumor growth. Interestingly, the peptibody recognizes both S100A8 and S100A9 proteins on the surface of MDSCs. We also found that Eritoran or anti-S100A8 neutralizing antibodies suppressed tumor growth (Figures 5b and 8a).

S100A8 and/or S100A9 appears to be found under inflammatory stimuli in microvascular endothelial cells in mice,[16] or humans.[15] We previously reported that tumor-derived growth factors such as TNFα and vascular endothelial growth factor-induced endogenous TLR4 ligands. In the present study, mRNA levels of TNFα, IL6, S100A8 and Ccl2 in primary tumor sites were reduced by Eritoran (data not shown), suggesting that positive feedback loop on TLR4/MD-2 activation can occur in primary tumor sites. In addition, Cxcl1 is known to regulate positively S100A8/S100A9 autocrine loop, CXCR2 antagonist can be used for combination with chemotherapy.[51] As similar to a CXCR2 antagonist, we found that Eritoran is also able to diminish TNFα production in tumor-associated host cells. Thus, the blockade of TLR4/MD-2 can be a putative clinical target at early phase with chemotherapy, and other inflammatory-mediated diseases. In addition, TLR4 expression in breast cancer is implicated in paxlitaxel chemoresistance.[67] Thus, the functional inhibition of TLR4, or targeting the ligand is presumably useful for a combination therapy with other chemotherapeutic agents.

Taken together, we conclude that S100A8 directly binds to TLR4/MD-2 through C-terminal region, and that S100A8-mediated TLR4 signaling contributes to establishing tumor microenvironment.

MATERIALS AND METHODS

Chemicals and antibodies

LPS (*Escherichia coli*, 055:B5) was purchased from Sigma (St. Louis, MO, USA). Rabbit polyclonal anti-phospho-p38 (9211), anti-p38 (9212), rabbit monoclonal anti-phospho-p65 (3033) and anti-p65 (8242) antibodies were from Cell Signaling Technology (Danvers, MA, USA). Anti-β-actin (013-24553) monoclonal antibody was purchased from WAKO Pure Chemical (Osaka, Japan). S100A8 (2–89; full length of mouse S100A8), S100A8 (2–31), S100A8 (31–60) and S100A8 (60–89) were synthesized by Scrum (Tokyo, Japan), or Thermo Fisher (Waltham, MA, USA) (97.7% purity by high-performance liquid chromatography analysis). Mammalian cell-derived S100A8 protein was prepared as described in previously.[68] The purity of recombinant proteins was above 98% as judged by SDS–polyacrylamide gel electrophoresis analysis. Endotoxin levels determined by LAL test (WAKO Pure Chemical) were < 0.05 EU/μg. Recombinant RAGE protein was purchased from R&D systems (Minneapolis, MN, USA). Eritoran was kindly provided from Eisai Inc (Andover, MA, USA). Mouse mammary 4T1 tumor cells were purchased from ATCC (Manassas, VA, USA). The E0771 breast cancer cell line was originally established by Dr Sirotnak (Memorial Sloan-Kettering Cancer Center, New York, NY, USA) and was kindly provided by Dr Mihich (Roswell Park Memorial Institute, Buffalo, NY, USA).[69] All cell lines were checked every two months, and found to be mycoplasma free.

Generation of S100A8 antibodies

His-tagged mouse S100A8 recombinant proteins were generated in pET30a (Novagen, Madison, WI, USA). The recombinant proteins were *E. coli* BL21 cells and purified on the TALON metal affinity resins (Clontech, Mountain View, CA, USA). Japanese white rabbits were immunized against His-tagged S100A8 protein. Antibody titration was determined by enzyme immunoassay every week. Anti-S100A8 antibodies were purified on the protein A sepharose beads (GE Healthcare, Waukesha, WI, USA), and eluted with 0.1-M glycine (pH 2.7), followed by neutralizing with 1-M Tris-HCl (pH 9.0). The purified antibody was desalted in phosphate-buffered saline with PD-10 desalting columns (GE Healthcare). The activity of neutralizing against S100A8 was optimized on a cell migration assay under S100A8 stimulation.

In vitro migration assay

Murine peritoneal macrophages were harvested 4 days after an i.p. injection of 800 μl of 10% thioglycollate broth (TGC). TGC-elicited peritoneal macrophages were recovered by injecting phosphate-buffered saline. The migration of RAW264.7, LLC cells or peritoneal macrophages was evaluated using a culture insert (BD Falcon, Franklin Lakes, NJ, USA) in Dulbecco's Modified Eagle Medium supplemented with 0.1% bovine serum albumin. Cells were added into the upper well of the culture insert (8 μm pore size, BD Falcon) and the indicated peptides were added to the lower wells. An aliquot (200 μl) of the cell suspension (5×10^4 cells per well) was seeded in each of the upper wells and incubated for 6 h at 37 °C with 5% CO_2. Cells that migrated through the filter were counted with crystal violet staining.

Quantitative-PCR analysis

Cells were treated with S100A8 in Dulbecco's Modified Eagle Medium supplemented with 0.1% bovine serum albumin for cytokine induction. Total RNA was extracted using RNeasy Plus Mini Kit (Qiagen, Valencia, CA, USA). Complementary DNA was synthesized with PrimeScript 1st Strand cDNA Synthesis Kit (TAKARA Bio, Otsu, Japan). Quantitative-PCR analysis was carried out using PowerSybr Green mixture (Life Technologies, Carlsbad, CA, USA) and StepOnePlus Real-Time PCR System (Life Technologies). Gene expression levels were calculated from Ct values, and the relationship between the Ct value and a logarithm of the copy number of a target gene was confirmed to be on a linear line using the corresponding isolated DNA and its serial dilutions as a standard. Thus, gene expression levels for Il-6, Tnfα, Saa3, S100a8, Arg-1 and Ccl2 were normalized against that of β-actin in each sample. The following primers were used; β-actin, 5′-TTCTTTGCAGCTCCTTCGTT-3′ and 5′-ATG GAGGGGAATACAGCCC-3′; Il-6, 5′-AACGATGATGCACTTGCAGA-3′ and 5′-TG GTACTCCAGAAGACCAGAGG-3′; Tnfα, 5′-ATGAGAGGGAGGCCATTTG-3′ and 5′-CAGCCTCTTCTCATTCCTGC-3′; Ccl2, 5′-GGGATCATCTTGCTGGTGAA-3′ and 5′-AGGTCCCTGTCATGCTTCTG-3′; Saa3, 5′-CCCGAGCATGGAAGTATTT G-3′ and 5′-GTTGACAGCCAAAGATGGGT-3′; S100a8, 5′-CCGTCTTCAAGACATCG TTTGA-3′ and 5′- GTAGAGGGCATGGTGATTTCCT-3′; and Arg-1, 5′-CATGA GCTCCAAGCCAAAGT-3′ and 5′-TTTTTCCAGCAGACCAGCTT-3′.

ELISA assay

TLR4/MD-2 or MD-2 recombinant proteins were purified as previously reported.[28,70] These proteins were coated on high-binding ELISA plate (Greiner, Frickenhausen, Germany), followed by blocking with protein-free blocking buffer (Thermo Fisher). S100A8 at various concentrations were then added to the receptor-coated ELISA plates. For peptide coating, the polylactate strip plates (Greiner) were used. The TLR4/MD-2 recombinant proteins at various concentrations were added to the plate. Each plate was incubated with anti-S100A8 or anti-TLR4 antibodies. The plates were washed, incubated with the secondary antibody conjugated Horseradish peroxidase, followed by the addition of substrate. The reaction was stopped by the addition of 0.2-N H_2SO_4 solutions. Absorbance at OD_{450} was measured by a microplate reader (Thermo Fisher).

Computational simulations of TLR4/MD-2-S100A8 complex

The complex structure models (decoys) were generated from the crystal structures of TLR4/MD-2 monomer and S100A8 dimer by the combination of rigid-body docking program ZDOCK 3,[71,72] and clustering/reranking method CyClus.[48] For a given orientation of one protein relative to the other fixed protein optimal translational positions were determined using a fast-Fourier transform-based method and highest-scoring structure with desolvation energy, electrostatic energy and shape complementarity was stored. A total of 54 000 decoy structures were generated with a 6° increment in rotational space by ZDOCK and reranked by CyClus. CyClus can perform a fast clustering using a cylindrical approximation of interface and has been shown to improve the results of ZDOCK in many cases.[48] The monomer structure of TLR4/MD-2 and the homodimer structure of S100A8 were taken from the Protein Data Bank (PDB); TLR4/MD-2 (PDB: 2Z64) and S100A8 (PDB: 1MR8). After docking and reranking, decoy structures with

Table 2. Properties of top five models for TLR4/MD-2/human S100A8 dimer

Id	*Rank* CyClus	*Rank* ZDOCK	*Score* ZDOCK
1	2	9	1364
2	3	15	1338
3	4	18	1311
4	5	73	1222
5	6	88	1214

S100A8 located on the dimerization interface of TLR4/MD-2 were excluded referring to LPS bound form of TLR4/MD-2 dimer (PDB: 3VQ2). In this process, the highest ranked structure was excluded. Finally top five models (Table 2) were examined as plausible complex structures.

Western blotting

Cells were lysed in the lysis buffer (50-mM Tris-HCl (pH 7.4), 150-mM NaCl, 5-mM $Na_4P_2O_7$, 10-mM β-glycerophosphate, 1-mM EDTA, 1-mM EGTA and 1% (v/v) Triton X-100) containing the Complete Mini protease inhibitor cocktail (Roche, Indianapolis, IN, USA) and the PhosSTOP phosphatase inhibitor cocktail (Roche). Cell lysates (20 μg) were separated by SDS–polyacrylamide gel electrophoresis and transferred to an Immobilon P membrane (Millipore, Billerica, MA, USA). After blocking with Blocking One or Blocking One-P (Nacalai Tesque, Kyoto, Japan), the membranes were probed with the indicated antibody, followed by Horseradish peroxidase-conjugated anti-rabbit IgG or anti-mouse IgG (GE Healthcare). Signals were visualized by SuperSignal West Pico Chemiluminescent Substrate (Thermo Fisher).

Animal study

C57BL/6 J mice were purchased from Clea Japan Inc. (Tokyo, Japan) and *Tlr4*$^{-/-}$, *MyD88*$^{-/-}$ mice were purchased from Oriental Bioservice, Inc (Kyoto, Japan). MD-2$^{-/-}$ mice were provided by RIKEN.[73] Mice were used for experiments at 2–3 months of age. For Lewis lung cancer implantation mouse model, LLC cells were subcutaneously implanted into male C57BL/6 J mice. After 10 days, the size-matched tumor-bearing mice are randomly divided into two groups. One goup received Eritoran (5 mg/kg, i.p.), and the other received 5% dextrose water alone once daily for five consecutive days. For treatment with anti-S100A8 neutralizing antibodies, tumor-bearing mice received anti-S100A8 antibodies every 2 days for five consecutive days. Normal rabbit IgG obtained from pre-immune serum was used as a control. For 4T1 and E0771 implantation models, BALB/c and C57BL6J female mice were used respectively. Mice were killed, and minced mouse lungs or tumors were digested with collagenase/dispase/DNase solution. Collected cells were pretreated with anti-CD16/CD32 (BD Biosciences, San Jose, CA, USA; 553142), and then incubated with anti-CD11b-FITC (BD Biosciences; 557396), anti-Ly6G-PE (BD Biosciences; 551460) and anti-Ly6C-APC (BD Biosciences; 560595) antibodies, and analyzed by flow cytometry (Beckman Coulter, Fullerton, CA, USA; Cytomics FC500). For TAM staining, anti-CD11b-FITC and anti-F4/80 PE (eBioscience, San Diego, CA, USA; 12-4801) were used. For CD4/CD8 staining, anti-CD4-FITC (BD Biosciences; 553046) and anti-CD8-PE (BD Biosciences; 553032) were used. To determine tumor volume, the longitudinal diameter (length) and the transverse diameter (width) were determined. Tumor volume based on measurements by vernier calipers were calculated as Tumor volume = 1/2(length × width).[50] All procedures performed with mice were approved by the Animal Research Committee of Tokyo Women's Medical University.

Immunohistochemistry

To immunostain tumor vasculatures, the cryo sections (6 μm) obtained from frozen primary tumors, were incubated with anti-CD31 (BD Pharmingen, San Jose, CA, USA; 550274), and/or anti-α-smooth muscle actin (DAKO, Carpinteria, CA, USA; M0851) followed by AlexaFlour 488-conjugated rat IgG and/or AlexaFlour 555-conjugated mouse IgG secondary antibodies (Molecular Probes, Eugene, OR, USA) were used to visualize the signals by a fluorescent microscopy (BIOREVO BZ-9000; KEYENCE, Osaka, Japan) or a confocal microscope (LSM-710; Carl Zeiss, Oberkochen, Germany). DAPI staining was used for nuclear staining.

Statistical analysis

Data are shown as the mean ± s.d. Statistical significance analysis was completed by the two-sided Student's *t*-test assuming the equal variance of the test, or Mann–Whitney U test (GraphPad Prism 6.0 Software, San Diego, CA, USA). *P*-values < 0.05 were considered statistically significant. In all the figures, levels of statistical significance are indicated as $^{*}P < 0.05$, $^{**}P < 0.01$.

CONFLICT OF INTEREST

The authors declare no conflict of interest.

ACKNOWLEDGEMENTS

We thank Drs Hiroyuki Aburatani and Akira Watanabe (Genome Science Division, Research Center for Advanced Science and Technology, The University of Tokyo) for providing an expression system for mammalian cell-derived S100A8, and Dr Mihich (Roswell Park Cancer Institute, NY, USA) for providing E0771 cells. We thank Dr Tatsuya Shimizu (Institute of Advanced Biomedical Engineering and Science, Tokyo Women's Medical University) for cell sorting technology. We also thank Dr Sachie Hiratsuka for valuable discussion and Messr. Tsutomu Omori and Taishi Mishima for technical assistance. This work was supported by Grants-in-Aid for Scientific Research from the Ministry of Education, Culture, Sports, Science and Technology of Japan (to YM, 21117008) (to AD, 24501321) (to TT, 26440063).

REFERENCES

1 Donato R. Functional roles of S100 proteins, calcium-binding proteins of the EF-hand type. *Biochim Biophys Acta* 1999; **1450**: 191–231.
2 Schafer BW, Heizmann CW. The S100 family of EF-hand calcium-binding proteins: functions and pathology. *Trends Biochem Sci* 1996; **21**: 134–140.
3 Hunter MJ, Chazin WJ. High level expression and dimer characterization of the S100 EF-hand proteins, migration inhibitory factor-related proteins 8 and 14. *J Biol Chem* 1998; **273**: 12427–12435.
4 Vogl T, Leukert N, Barczyk K, Strupat K, Roth J. Biophysical characterization of S100A8 and S100A9 in the absence and presence of bivalent cations. *Biochim Biophys Acta* 2006; **1763**: 1298–1306.
5 Grimbaldeston MA, Geczy CL, Tedla N, Finlay-Jones JJ, Hart PH. S100A8 induction in keratinocytes by ultraviolet A irradiation is dependent on reactive oxygen intermediates. *J Invest Dermatol* 2003; **121**: 1168–1174.
6 Kumar RK, Yang Z, Bilson S, Thliveris S, Cooke BE, Geczy CL. Dimeric S100A8 in human neutrophils is diminished after phagocytosis. *J Leukoc Biol* 2001; **70**: 59–64.
7 Ryckman C, Vandal K, Rouleau P, Talbot M, Tessier PA. Proinflammatory activities of S100: proteins S100A8, S100A9, and S100A8/A9 induce neutrophil chemotaxis and adhesion. *J Immunol* 2003; **170**: 3233–3242.
8 Hessian PA, Edgeworth J, Hogg N. MRP-8 and MRP-14, two abundant Ca(2+)-binding proteins of neutrophils and monocytes. *J Leukoc Biol* 1993; **53**: 197–204.
9 Kumar A, Steinkasserer A, Berchtold S. Interleukin-10 influences the expression of MRP8 and MRP14 in human dendritic cells. *Int Arch Allergy Immunol* 2003; **132**: 40–47.
10 Healy AM, Pickard MD, Pradhan AD, Wang Y, Chen Z, Croce K *et al.* Platelet expression profiling and clinical validation of myeloid-related protein-14 as a novel determinant of cardiovascular events. *Circulation* 2006; **113**: 2278–2284.
11 Zreiqat H, Howlett CR, Gronthos S, Hume D, Geczy CL. S100A8/S100A9 and their association with cartilage and bone. *J Mol Histol* 2007; **38**: 381–391.
12 Passey RJ, Williams E, Lichanska AM, Wells C, Hu S, Geczy CL *et al.* A null mutation in the inflammation-associated S100 protein S100A8 causes early resorption of the mouse embryo. *J Immunol* 1999; **163**: 2209–2216.
13 Hsu K, Passey RJ, Endoh Y, Rahimi F, Youssef P, Yen T *et al.* Regulation of S100A8 by glucocorticoids. *J Immunol* 2005; **174**: 2318–2326.
14 Xu K, Yen T, Geczy CL. Il-10 up-regulates macrophage expression of the S100 protein S100A8. *J Immunol* 2001; **166**: 6358–6366.
15 McCormick MM, Rahimi F, Bobryshev YV, Gaus K, Zreiqat H, Cai H *et al.* S100A8 and S100A9 in human arterial wall. Implications for atherogenesis. *J Biol Chem* 2005; **280**: 41521–41529.
16 Yen T, Harrison CA, Devery JM, Leong S, Iismaa SE, Yoshimura T *et al.* Induction of the S100 chemotactic protein, CP-10, in murine microvascular endothelial cells by proinflammatory stimuli. *Blood* 1997; **90**: 4812–4821.
17 Eckert RL, Broome AM, Ruse M, Robinson N, Ryan D, Lee K. S100 proteins in the epidermis. *J Invest Dermatol* 2004; **123**: 23–33.

18 Rahimi F, Hsu K, Endoh Y, FGF-2 Geczy CL. IL-1beta and TGF-beta regulate fibroblast expression of S100A8. *FEBS J* 2005; **272**: 2811–2827.
19 Kitamura T, Fujishita T, Loetscher P, Revesz L, Hashida H, Kizaka-Kondoh S *et al.* Inactivation of chemokine (C-C motif) receptor 1 (CCR1) suppresses colon cancer liver metastasis by blocking accumulation of immature myeloid cells in a mouse model. *Proc Natl Acad Sci USA* 2010; **107**: 13063–13068.
20 Kerkhoff C, Nacken W, Benedyk M, Dagher MC, Sopalla C, Doussiere J. The arachidonic acid-binding protein S100A8/A9 promotes NADPH oxidase activation by interaction with p67phox and Rac-2. *FASEB J* 2005; **19**: 467–469.
21 Vogl T, Ludwig S, Goebeler M, Strey A, Thorey IS, Reichelt R *et al.* MRP8 and MRP14 control microtubule reorganization during transendothelial migration of phagocytes. *Blood* 2004; **104**: 4260–4268.
22 Rammes A, Roth J, Goebeler M, Klempt M, Hartmann M, Sorg C. Myeloid-related protein (MRP) 8 and MRP14, calcium-binding proteins of the S100 family, are secreted by activated monocytes via a novel, tubulin-dependent pathway. *J Biol Chem* 1997; **272**: 9496–9502.
23 Ehrchen JM, Sunderkotter C, Foell D, Vogl T, Roth J. The endogenous Toll-like receptor 4 agonist S100A8/S100A9 (calprotectin) as innate amplifier of infection, autoimmunity, and cancer. *J Leukoc Biol* 2009; **86**: 557–566.
24 Vabulas RM, Ahmad-Nejad P, da Costa C, Miethke T, Kirschning CJ, Hacker H *et al.* Endocytosed HSP60s use toll-like receptor 2 (TLR2) and TLR4 to activate the toll/interleukin-1 receptor signaling pathway in innate immune cells. *J Biol Chem* 2001; **276**: 31332–31339.
25 Asea A, Rehli M, Kabingu E, Boch JA, Bare O, Auron PE *et al.* Novel signal transduction pathway utilized by extracellular HSP70: role of toll-like receptor (TLR) 2 and TLR4. *J Biol Chem* 2002; **277**: 15028–15034.
26 Yang H, Hreggvidsdottir HS, Palmblad K, Wang H, Ochani M, Li J *et al.* A critical cysteine is required for HMGB1 binding to Toll-like receptor 4 and activation of macrophage cytokine release. *Proc Natl Acad Sci USA* 2010; **107**: 11942–11947.
27 Vogl T, Tenbrock K, Ludwig S, Leukert N, Ehrhardt C, van Zoelen MA *et al.* Mrp8 and Mrp14 are endogenous activators of Toll-like receptor 4, promoting lethal, endotoxin-induced shock. *Nat Med* 2007; **13**: 1042–1049.
28 Deguchi A, Tomita T, Omori T, Komatsu A, Ohto U, Takahashi S *et al.* Serum amyloid A3 binds MD-2 to activate p38 and NF-kappaB pathways in a MyD88-dependent manner. *J Immunol* 2013; **191**: 1856–1864.
29 Hiratsuka S, Watanabe A, Sakurai Y, Akashi-Takamura S, Ishibashi S, Miyake K *et al.* The S100A8-serum amyloid A3-TLR4 paracrine cascade establishes a pre-metastatic phase. *Nat Cell Biol* 2008; **10**: 1349–1355.
30 Pal D, Dasgupta S, Kundu R, Maitra S, Das G, Mukhopadhyay S *et al.* Fetuin-A acts as an endogenous ligand of TLR4 to promote lipid-induced insulin resistance. *Nat Med* 2012; **18**: 1279–1285.
31 Biragyn A, Ruffini PA, Leifer CA, Klyushnenkova E, Shakhov A, Chertov O *et al.* Toll-like receptor 4-dependent activation of dendritic cells by beta-defensin 2. *Science* 2002; **298**: 1025–1029.
32 Smiley ST, King JA, Hancock WW. Fibrinogen stimulates macrophage chemokine secretion through toll-like receptor 4. *J Immunol* 2001; **167**: 2887–2894.
33 Okamura Y, Watari M, Jerud ES, Young DW, Ishizaka ST, Rose J *et al.* The extra domain A of fibronectin activates Toll-like receptor 4. *J Biol Chem* 2001; **276**: 10229–10233.
34 Jiang D, Liang J, Fan J, Yu S, Chen S, Luo Y *et al.* Regulation of lung injury and repair by Toll-like receptors and hyaluronan. *Nat Med* 2005; **11**: 1173–1179.
35 Johnson GB, Brunn GJ, Kodaira Y, Platt JL. Receptor-mediated monitoring of tissue well-being via detection of soluble heparan sulfate by Toll-like receptor 4. *J Immunol* 2002; **168**: 5233–5239.
36 Schaefer L, Babelova A, Kiss E, Hausser HJ, Baliova M, Krzyzankova M *et al.* The matrix component biglycan is proinflammatory and signals through Toll-like receptors 4 and 2 in macrophages. *J Clin Invest* 2005; **115**: 2223–2233.
37 Merline R, Moreth K, Beckmann J, Nastase MV, Zeng-Brouwers J, Tralhao JG *et al.* Signaling by the matrix proteoglycan decorin controls inflammation and cancer through PDCD4 and MicroRNA-21. *Sci Signal* 2011; **4**: ra75.
38 Kawai T, Akira S. The role of pattern-recognition receptors in innate immunity: update on Toll-like receptors. *Nat Immunol* 2010; **11**: 373–384.
39 Park BS, Song DH, Kim HM, Choi BS, Lee H, Lee JO. The structural basis of lipopolysaccharide recognition by the TLR4-MD-2 complex. *Nature* 2009; **458**: 1191–1195.
40 Doyle SL, O'Neill LA. Toll-like receptors: from the discovery of NFkappaB to new insights into transcriptional regulations in innate immunity. *Biochem Pharmacol* 2006; **72**: 1102–1113.
41 Fitzgerald KA, Rowe DC, Barnes BJ, Caffrey DR, Visintin A, Latz E *et al.* LPS-TLR4 signaling to IRF-3/7 and NF-kappaB involves the toll adapters TRAM and TRIF. *J Exp Med* 2003; **198**: 1043–1055.
42 Kim HM, Park BS, Kim JI, Kim SE, Lee J, Oh SC *et al.* Crystal structure of the TLR4-MD-2 complex with bound endotoxin antagonist Eritoran. *Cell* 2007; **130**: 906–917.
43 Tomita T, Sakurai Y, Ishibashi S, Maru Y. Imbalance of Clara cell-mediated homeostatic inflammation is involved in lung metastasis. *Oncogene* 2011; **30**: 3429–3439.
44 Hiratsuka S, Watanabe A, Aburatani H, Maru Y. Tumour-mediated upregulation of chemoattractants and recruitment of myeloid cells predetermines lung metastasis. *Nat Cell Biol* 2006; **8**: 1369–1375.
45 Propper C, Huang X, Roth J, Sorg C, Nacken W. Analysis of the MRP8-MRP14 protein-protein interaction by the two-hybrid system suggests a prominent role of the C-terminal domain of S100 proteins in dimer formation. *J Biol Chem* 1999; **274**: 183–188.
46 Bjork P, Bjork A, Vogl T, Stenstrom M, Liberg D, Olsson A *et al.* Identification of human S100A9 as a novel target for treatment of autoimmune disease via binding to quinoline-3-carboxamides. *PLoS Biol* 2009; **7**: e97.
47 Riva M, Kallberg E, Bjork P, Hancz D, Vogl T, Roth J *et al.* Induction of nuclear factor-kappaB responses by the S100A9 protein is Toll-like receptor-4-dependent. *Immunology* 2012; **137**: 172–182.
48 Omori S, Kitao A. CyClus: a fast, comprehensive cylindrical interface approximation clustering/reranking method for rigid-body protein-protein docking decoys. *Proteins* 2013; **81**: 1005–1016.
49 Chen K, Huang J, Gong W, Iribarren P, Dunlop NM, Wang JM. Toll-like receptors in inflammation, infection and cancer. *Int Immunopharmacol* 2007; **7**: 1271–1285.
50 Akira S. Mammalian Toll-like receptors. *Curr Opin Immunol* 2003; **15**: 5–11.
51 Acharyya S, Oskarsson T, Vanharanta S, Malladi S, Kim J, Morris PG *et al.* A CXCL1 paracrine network links cancer chemoresistance and metastasis. *Cell* 2012; **150**: 165–178.
52 Gabrilovich DI, Nagaraj S. Myeloid-derived suppressor cells as regulators of the immune system. *Nat Rev Immunol* 2009; **9**: 162–174.
53 Ichikawa M, Williams R, Wang L, Vogl T, Srikrishna G. S100A8/A9 activate key genes and pathways in colon tumor progression. *Mol Cancer Res* 2011; **9**: 133–148.
54 Hsu RY, Chan CH, Spicer JD, Rousseau MC, Giannias B, Rousseau S *et al.* LPS-induced TLR4 signaling in human colorectal cancer cells increases beta1 integrin-mediated cell adhesion and liver metastasis. *Cancer Res* 2011; **71**: 1989–1998.
55 Huang Y, Yuan J, Righi E, Kamoun WS, Ancukiewicz M, Nezivar J *et al.* Vascular normalizing doses of antiangiogenic treatment reprogram the immunosuppressive tumor microenvironment and enhance immunotherapy. *Proc Natl Acad Sci USA* 2012; **109**: 17561–17566.
56 Mantovani A, Allavena P. The interaction of anticancer therapies with tumor-associated macrophages. *J Exp Med* 2015; **212**: 435–445.
57 Kaplan RN, Riba RD, Zacharoulis S, Bramley AH, Vincent L, Costa C *et al.* VEGFR1-positive haematopoietic bone marrow progenitors initiate the pre-metastatic niche. *Nature* 2005; **438**: 820–827.
58 Kawasaki K, Akashi S, Shimazu R, Yoshida T, Miyake K, Nishijima M. Involvement of TLR4/MD-2 complex in species-specific lipopolysaccharide-mimetic signal transduction by Taxol. *J Endotoxin Res* 2001; **7**: 232–236.
59 Ghavami S, Rashedi I, Dattilo BM, Eshraghi M, Chazin WJ, Hashemi M *et al.* S100A8/A9 at low concentration promotes tumor cell growth via RAGE ligation and MAP kinase-dependent pathway. *J Leukoc Biol* 2008; **83**: 1484–1492.
60 Turovskaya O, Foell D, Sinha P, Vogl T, Newlin R, Nayak J *et al.* RAGE, carboxylated glycans and S100A8/A9 play essential roles in colitis-associated carcinogenesis. *Carcinogenesis* 2008; **29**: 2035–2043.
61 Szajnik M, Szczepanski MJ, Czystowska M, Elishaev E, Mandapathil M, Nowak-Markwitz E *et al.* TLR4 signaling induced by lipopolysaccharide or paclitaxel regulates tumor survival and chemoresistance in ovarian cancer. *Oncogene* 2009; **28**: 4353–4363.
62 Szczepanski MJ, Czystowska M, Szajnik M, Harasymczuk M, Boyiadzis M, Kruk-Zagajewska A *et al.* Triggering of Toll-like receptor 4 expressed on human head and neck squamous cell carcinoma promotes tumor development and protects the tumor from immune attack. *Cancer Res* 2009; **69**: 3105–3113.
63 Volk-Draper L, Hall K, Griggs C, Rajput S, Kohio P, DeNardo D *et al.* Paclitaxel therapy promotes breast cancer metastasis in a TLR4-dependent manner. *Cancer Res* 2014; **74**: 5421–5434.
64 Andreani V, Gatti G, Simonella L, Rivero V, Maccioni M. Activation of Toll-like receptor 4 on tumor cells *in vitro* inhibits subsequent tumor growth *in vivo*. *Cancer Res* 2007; **67**: 10519–10527.
65 Shi C, Jia T, Mendez-Ferrer S, Hohl TM, Serbina NV, Lipuma L *et al.* Bone marrow mesenchymal stem and progenitor cells induce monocyte emigration in response to circulating toll-like receptor ligands. *Immunity* 2011; **34**: 590–601.

66 Qin H, Lerman B, Sakamaki I, Wei G, Cha SC, Rao SS *et al.* Generation of a new therapeutic peptide that depletes myeloid-derived suppressor cells in tumor-bearing mice. *Nat Med* 2014; **20**: 676–681.
67 Rajput S, Volk-Draper LD, Ran S. TLR4 is a novel determinant of the response to paclitaxel in breast cancer. *Mol Cancer Ther* 2013; **12**: 1676–1687.
68 Hiratsuka S, Ishibashi S, Tomita T, Watanabe A, Akashi-Takamura S, Murakami M *et al.* Primary tumours modulate innate immune signalling to create pre-metastatic vascular hyperpermeability foci. *Nat Commun* 2013; **4**: 1853.
69 Ewens A, Mihich E, Ehrke MJ. Distant metastasis from subcutaneously grown E0771 medullary breast adenocarcinoma. *Anticancer Res* 2005; **25**: 3905–3915.
70 Ohto U, Fukase K, Miyake K, Shimizu T. Structural basis of species-specific endotoxin sensing by innate immune receptor TLR4/MD-2. *Proc Natl Acad Sci USA* 2012; **109**: 7421–7426.
71 Chen R, Li L, Weng Z. ZDOCK: an initial-stage protein-docking algorithm. *Proteins* 2003; **52**: 80–87.
72 Pierce BG, Hourai Y, Weng Z. Accelerating protein docking in ZDOCK using an advanced 3D convolution library. *PLoS One* 2011; **6**: e24657.
73 Nagai Y, Akashi S, Nagafuku M, Ogata M, Iwakura Y, Akira S *et al.* Essential role of MD-2 in LPS responsiveness and TLR4 distribution. *Nat Immunol* 2002; **3**: 667–672.

Supplementary Information accompanies this paper on the Oncogene website (http://www.nature.com/onc)